 Bull. Chem. Soc. Jpn., 75, 909–917 (2002)

Headline Articles

Femtosecond Mid-Infrared Pump–Probe Study of Wave Packet Motion in a Medium-Strong Intramolecular Hydrogen Bond

Dorte Madsen,[#] Jens Stenger, Jens Dreyer, Peter Hamm, Erik T. J. Nibbering,[*] and Thomas Elsaesser

Max Born Institut für Nichtlineare Optik und Kurzzeitspektroskopie, Max Born Strasse 2A, D-12489 Berlin, Germany

(Received September 28, 2001)

We inspect the O–H stretching vibration of the medium-strong hydrogen bond in phthalic acid monomethyl ester in nonpolar solution by use of single-colour spectrally integrated femtosecond mid-infrared spectroscopy. We derive amplitude and phase characteristics of the coherent modulations of the pump-probe signals as a function of excitation wavelength. We exclude the role of Fermi resonances in the oscillatory contribution to the pump–probe signals. The observed periodic feature is due to wave packet motion of an underdamped out-of-plane 100 cm^{-1} mode that modulates the hydrogen bond distance. This low-frequency mode anharmonically coupled to the O–H stretching vibration is impulsively excited by the ultrashort mid-infrared pump pulse.

Hydrogen bonds form a special class of interaction where a hydrogen atom is shared between two electronegative atoms of the donor and accceptor groups. The charge distribution in this three atom chemical bond is crucial for its special properties, amongst which the strength lies somewhere between covalent and ionic bonds. Infrared spectroscopy is one of the most important spectroscopic tools to determine the properties of specific hydrogen bonds.[1] In particular, a direct correlation between the hydrogen bond distance and the frequency of the O–H or N–H stretching modes has been shown to exist. In this case the magnitude of the red-shift of these vibrational resonances is a direct indication of the hydrogen bond strength. This is illustrated in Fig. 1, where the O–H vibrational bands are shown for the case of the free O–H group of phenol in C_2Cl_4, for the weak hydrogen bond of HOD in D_2O and for the medium-strong hydrogen bond in phthalic acid monomethyl ester (PMME) in C_2Cl_4. Other marked features include the increase in intensity and the presence of substructure of the O–H or N–H stretching bands.

Numerous theoretical studies of the O–H stretching vibrational line shape have used the concept of anharmonic coupling between vibrational normal modes.[2–4] Here it is assumed that the vibrational Hamiltonian describing the O–H stretching line shape in a hydrogen bond can be decomposed into harmonic oscillators denoting the O–H (or O–D) stretching normal mode (typically located in the 2000–3500 cm^{-1} frequency range), and one (or more) low-frequency mode(s), like the hydrogen bond O···O stretching and bending vibrations, with typical eigenfrequencies of a few hundred wavenumbers, that modulate the hydrogen bond length. In addition to the harmonic position and momentum operators of these harmonic oscillators a coupling term is added that connects the motion of the high-frequency O–H stretching mode to those of the low-frequency modes. Other vibrational degrees of freedom, either intramolecular or intermolecular, when the molecule under consideration is immersed in a solvent, are treated phenomenologically by population relaxation and dephasing parameters. The effects of a distribution of hydrogen bond lengths and angles[5] can be implemented as well, resulting in a distribution of O–H frequencies upon hydrogen bonding. This type of line broadening can be expected for intermolecular hydrogen bonds, such as in water, where the flexibility allow for a broad range of geometric configurations, whereas for intramolecular hydrogen bonds, as happens to be the case for the molecule investigated in our present pump-probe study, often a more rigid hydrogen bond geometry occurs.

Usually an adiabatic separation of time scales between the motion of the fast O–H stretching mode and the slow O···O modes is made, where one can define potential energy surfaces for these slow modes as a function of the quantum state of the O–H stretching mode. From this it follows that the O–H stretching vibrational transition is accompanied by side-bands where the separation is given by the frequency of the slow modes, and the relative magnitude by Franck–Condon factors. The analogy with vibronic spectroscopy does not only apply for linear spectroscopy, but also extends to nonlinear spectroscopic techniques such as pump–probe and four-wave mixing. In the case of ultrashort pulse excitation with a spectral bandwidth larger than the interdistance between these side-

Current address: Department of Chemistry, Aarhus University, Langelandsgade 140, 8000 Aarhus C, Denmark

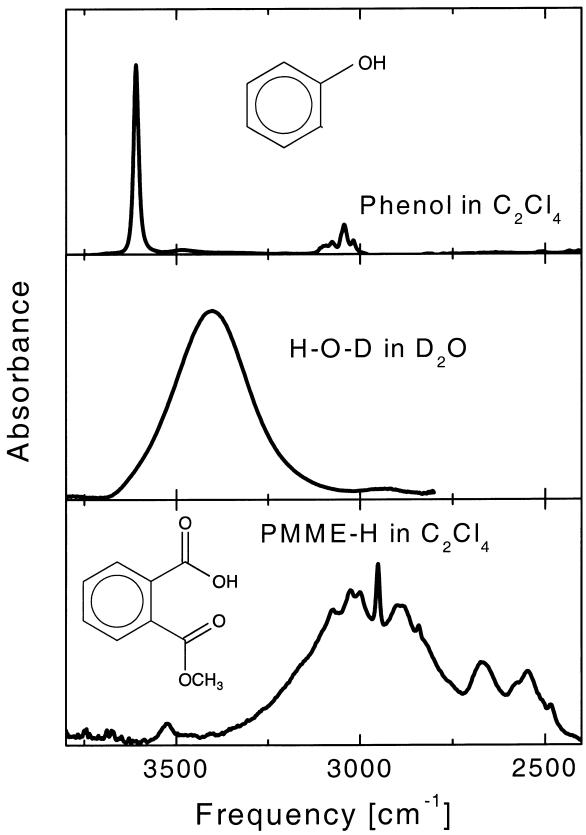

Fig. 1. Absorption spectra of the O–H stretching region of phenol in C_2Cl_4, HOD in D_2O, and PMME-H in C_2Cl_4. The free O–H group of phenol has a narrow vibrational transition at 3610 cm^{-1} with a width of 20 cm^{-1}. The O–H group in the weak hydrogen bond of HOD has a maximum at 3400 cm^{-1} and a width of 250 cm^{-1}. PMME-H with a medium-strong hydrogen bond has a O–H vibrational band that peaks at 3000 cm^{-1} and extends over 700 cm^{-1} with marked substructure.

bands, coherent excitation of several levels of these low-frequency modes occurs, with the generation of vibrational wave packets of these low-frequency modes as a consequence. These vibrational wave packets show up as coherent modulations in pump–probe and four wave mixing signals.

The fluctuating degrees of freedom of the solvent lead to perturbation of the phase properties of the O–H stretching oscillator, either by direct coupling of the O–H stretching mode with the electric field of the solvent, or indirectly by randomization of the motion of the low-frequency modes. These dephasing processes contribute to the extreme line broadening of the O–H stretching vibrational transitions in hydrogen bonded systems. With respect to four-wave mixing studies on the dephasing characteristics of the O–H stretching vibrational transitions we refer to recent work of our group on intermolecular (HOD in D_2O[6,7]) and intramolecular hydrogen bonds.[8]

When vibrational modes with higher frequencies such as the O–H bending mode, couple to the O–H stretching vibration,[9] one cannot make the adiabatic separation of time scales. Moreover, when overtone states such as the $v = 2$ state of the O–H bending mode, lie energetically near the $v = 1$ state of the O–H stretching vibration, one can expect the occurrence of Fermi resonances, with resulting splitting of transitions and dips (Evans windows) in absorption line shapes.[10,11] Coherent excitation of a transition split by a Fermi resonance would also lead to coherent modulations of pump–probe signals.

Recently we reported the coherent modulations of pump–probe signals of the deuterated derivative of a medium strong intramolecular hydrogen bonded molecular system, phthalic acid monomethyl ester (PMME-D).[12] The purpose of this paper is to explore further the characteristics of this wave packet generation in PMME. We show data for the ordinary protonated form, PMME-H, obtained with one-colour pump–probe spectroscopy with spectrally integrated (open band) detection, from which we demonstrate that the coherent modulation of the pump-probe signals occurs with the same frequency throughout the absorption band. Based on these results we demonstrate that a low frequency out-of-plane mode is responsible for the observed effects, whereas Fermi resonances with overtone states play a minor role. In addition we analyse the phase properties of the wave packet modulations and discuss those with respect to the known vibrational wave packet behaviour for vibronic transitions.

Experimental and Computational Methods

Femtosecond mid-infrared pulses were generated as described earlier.[13,14] In short, tunable mid-IR pulses with 130 fs duration, 150 cm^{-1} bandwidth and more than 1 μJ/pulse at 1 kHz repetition rate were produced by difference frequency mixing in $AgGaS_2$. Femtosecond IR pump-probe spectroscopy was performed by measuring the nonlinear transmission changes induced by the intense pump pulses, that are monitored by time delayed probe pulses, in itself replicas of the pump pulses. The pump intensity on the sample was 10^{10}–10^{11} W/cm^2, and the probe intensity was a factor of 0.04 lower. We observed a linear dependence of the pump–probe signals on pump intensity, and from this we may safely neglect multiphoton absorption contributions to the overall observations. Pump and probe pulses had the same polarisation.

The sample under study consisted of a solution of phthalic acid monomethyl ester (monomethyl phthalate, Aldrich, 97%) dissolved in C_2Cl_4 (Merck, extra pure) located in a 500 μm cell with 1 mm thick CaF_2-windows. Temporal spreading of the mid-IR pulses have been found to be negligible in our experiments.

Ground state geometry optimization and vibrational analysis of PMME was carried out by density functional theory using the B3LYP/6-31+G(d,p) method implemented in the program package GAUSSIAN98.[15] All calculated vibrational frequencies were scaled by a factor of 0.96.[16] Conformational analysis were performed with smaller basis sets (6-31G) by calculating potential energy surfaces for all relevant dihedral angles.

Results and Discussion

Structure of PMME-H. The optimized structure for the lowest energy conformer of PMME is shown in Fig. 2. Relevant geometry parameters, the absolute energy E and the dipole moment μ are indicated. PMME forms an intramolecular hydrogen bond between the O–H group of the carboxy substituent and the oxygen atom of the carbonyl group. The structure is quasi-planar. However, the hydrogen bond is part of a seven-membered ring that does not entirely fit into the plane of the benzene ring, so that the two substituents are somewhat tilted

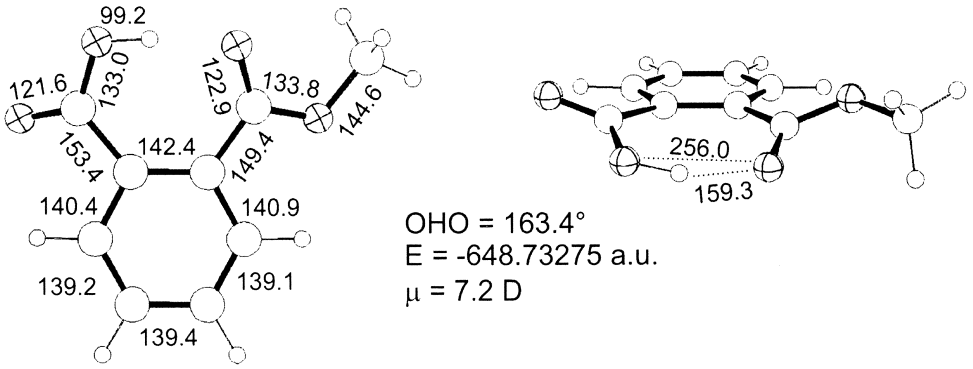

Fig. 2. Lowest energy conformer of PMME optimized by the B3LYP/6-31G+G(d,p) method. Bond lengths and hydrogen bond distances are specified in pm. The absolute energy E and the dipole moment μ are given. (large open spheres: C; small open spheres: H; crossed spheres: O).

out-of-plane. The methyl group is located quasi-in-plane pointing away from the benzene ring. The benzene bond involved in the seven-membered ring of the hydrogen bond is considerably stretched in comparison to the remaining benzene bonds which show standard aromatic C–C bond lengths. The heavy atom hydrogen bond O–O distance of 256.0 pm as well as the H···O distance of 159.3 pm indicate hydrogen bonds of intermediate strength.[17]

Further conformers with weaker hydrogen bonds as well as non-hydrogen-bonded conformers have been identified at higher energies. One hydrogen-bonded conformer lies about 1400 cm^{-1} higher in energy and involves a hydrogen bond to the methoxy oxygen atom. Another hydrogen-bonded conformer is identified about 6000 cm^{-1} higher in energy with a hydrogen bond to the carbonyl oxygen atom formed across the phenyl ring plane. Non-hydrogen bonded conformers have been calculated to be much less stable.

Steady State IR Spectra. IR spectra for PMME-H (Fig. 3A) and PMME-D (Fig. 3B) have been measured in C_2Cl_4 ($c = 5\times10^{-3}$ M) using CaF_2 windows and for PMME-H embedded in KBr (Fig. 3C). The pure solvent spectrum has been subtracted. Calculated spectra are shown in the lower panels. All vibrational frequencies are collected in Table 1. Above 1000 cm^{-1} the majority of bands can be assigned, whereas below 1000 cm^{-1} the assignment partly remains ambiguous.

The three modes that are dominated by the motion of the hydrogen or deuterium atom, repectively, involved in the H-bond exhibit major isotopic shifts (see Table 1). The calculated isotope shift for the O–H/O–D stretching mode 57 amounts to -839 cm^{-1}, the O–H/O–D in-plane deformation mode 40 shifts by -384 cm^{-1} (exp: -406 cm^{-1}), and the O–H/O–D out-of-plane deformation mode 24 shifts by -245 cm^{-1} (exp: -259 cm^{-1}). The hydrogen bond O···O stretching mode 10 is calculated to 343 cm^{-1} with a very small isotope shift of 1 cm^{-1}.

Below 200 cm^{-1}, which corresponds to the window where modes can be impulsively excited with our laser set-up, only 6 modes are located. Thereof only the mode 2 calculated to 69 cm^{-1} modulates the H-bond considerably. The isotope shift of this mode is calculated to 1 cm^{-1}.

Femtosecond IR Spectroscopy. We have performed one-colour pump–probe spectroscopy on the O–H stretching vibrational transition where the pulses have been tuned throughout the band (see Fig. 4). The resulting pump-probe transients are shown in Fig. 5 on a linear time scale and in Fig. 6 on a logarithmic scale. The spectrally-integrated transients obtained on PMME-H in C_2Cl_4 show similar features, but also differences, as seen in the spectrally-resolved data obtained on PMME-D, as reported recently.[12]

The solvent and cell window contributions to the signal (Fig. 5C) is more than an order of magnitude smaller. These signals are usually induced by cross-phase modulation effects through non-resonant $\chi^{(3)}$-interactions, and are only strongly present in spectrally dispersed detection schemes of the probe pulses. However, care has to be taken with this general remark when solvent overtone bands are present in the wavelength ranges under study.

The observed signals in Figs. 5 and 6 can thus safely be attributed to the molecule under study. Absorbance changes can be explained with the 5-level system as depicted in Fig. 7. Several remarks on nonlinear spectroscopy on vibrational transitions of hydrogen bonds have to be made. First, one has to take into account, besides the $v = 0$ and $v = 1$ levels, the vibrational overtone $v = 2$ state. In the case of pump–probe or four wave mixing spectroscopy one thus has to incorporate ground state bleach ($v = 0 \rightarrow v = 1$), stimulated emission ($v = 1 \rightarrow v = 0$) and excited-state absorption ($v = 1 \rightarrow v = 2$) contributions for the interpretation of the detected signals.[18] Because of anharmonicity of vibrations the excited-state absorption is red-shifted with respect to the ordinary transition. In addition, for the case of hydrogen bonded systems the occurrence of "hot" species after T_1-population relaxation of the $v = 1$ state have been reported, where the O–H stretching mode is in the $v = 0'$ ground state.[19] The importance of local heating effects have been noted before.[20] Often the collection of states along which the relaxation pathways occur have been described as an effective single "hot" ground state $v = 0'$, that subsequently relaxes back to the equilibrium $v = 0$ state on picosecond (or longer[8]) time scales. These transient "hot" states appear to exhibit vibrational transitions ($v = 0' \rightarrow v = 1'$) with frequencies blue shifted compared to the ordinary transition.

We observe all these features in the data shown in Figs. 5 and 6. Besides the ground-state bleach and stimulated emission contributions, the blue-shifted transient absorption is also

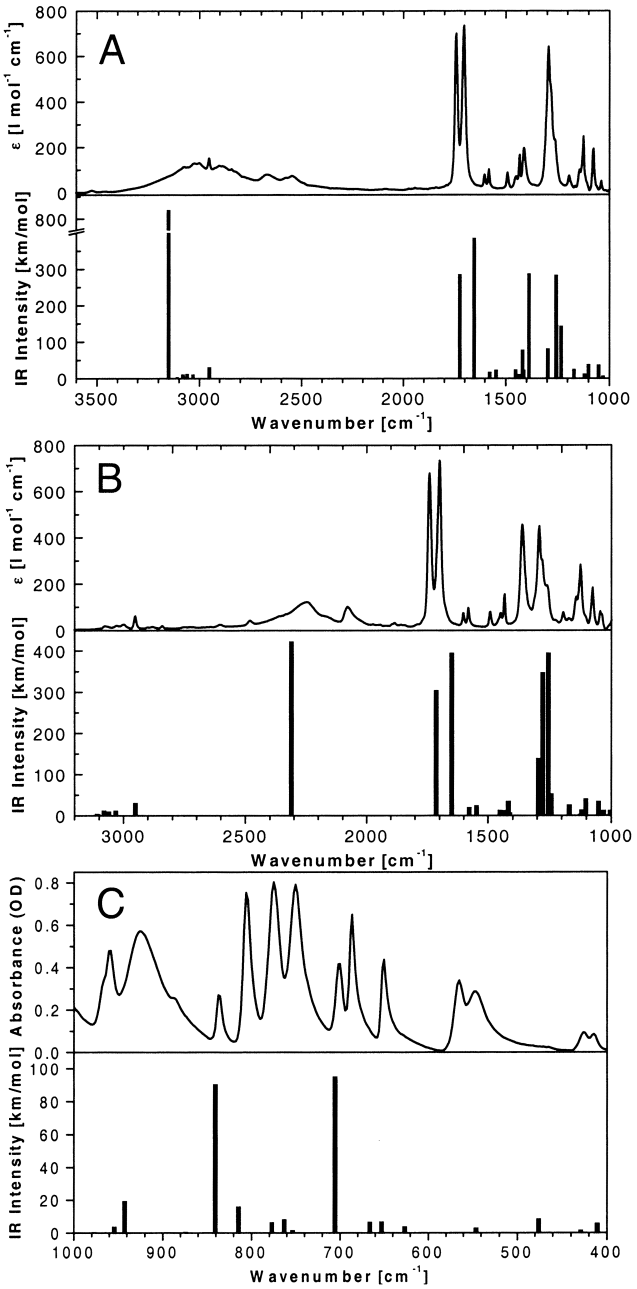

Fig. 3. Comparison of experimental (upper panels) and calculated (lower panels) IR spectra. (A) PMME-H in C_2Cl_4. (B) PMME-D in C_2Cl_4. (C) PMME-H in KBr.

clearly present, see, e.g., the transient observed at 3200 cm^{-1}. The appearance of this blue-shifted feature gives an indication of the T_1-relaxation time of the $v = 1$ state, that appears not longer than 200–250 fs, about half the value than reported for PMME-D.[12] A more precise number for T_1 cannot be given, since the appearance of the blue-shifted band is obscured by the coherent artifact contributions to the pump-probe signal.

The transient observed when the pulses were tuned at 2400 cm^{-1} might exhibit the excited-state absorption. The reason why the stimulated emission ($v = 1 \rightarrow v = 0$) contributes much less to the signal at 2400 cm^{-1} than the excited state absorption ($v = 1 \rightarrow v = 2$) lies in the fact that the transitions are centred at different frequency positions due to the anharmonic shift. Considering the signal-to-noise ratio, extraction of a more precise value for the T_1-relaxation time of the $v = 1$ state is unfortunately not possible. Two-colour pump-probe measurements should enable the elucidation of the lifetime of the O–H stretching mode in a more satisfying way. At longer delays we observe a non-exponential cooling behaviour back to the ground state equilibrium as shown in Fig. 6.

Finally, we note that rotational diffusion effects on the pump-probe signals can be discarded for the delay times under consideration. We measured an anisotropy decay for PMME-H in C_2Cl_4 in the time range of 20–30 ps, as can be expected for medium-sized molecules like PMME-H.[21]

Nature of the Coherent Signal in IR Pump–Probe. Superimposed to these incoherent contributions to the observed pump–probe signals coherent modulations are clearly observed. We now discuss whether the oscillatory contribution is due to band splitting because of Fermi resonances or to impulsive excitation of an anharmonically coupled low-frequency mode. In order to do this we inspect the amplitude and phase properties of these coherent modulations on the pump-probe signals (see Fig. 2). Analysis of the data after substraction of the overall decay curve using a decaying cosine term ($e^{-\gamma\tau}\cdot\cos[\omega\cdot\tau + \phi]$, where ω is the angular frequency of the out-of-plane mode, τ is the pulse delay, γ is the coherence decay rate, and ϕ is the phase of the oscillations) shows a continuous phase change around 3100 cm^{-1} where the total phase change amounts to 200–230 degrees when scanning through the O–H stretching band. The value for the coherence decay rate is $\gamma = 2 \pm 0.3$ ps^{-1}. We did not observe a frequency-dependence for γ within experimental accuracy.

The occurence of Fermi resonances between the O–H stretching $v = 1$ state and other vibrational states (such as the $v = 2$ state of the O–H bending mode) has often been proposed as a possible explanation for (part of) the substructure in O–H stretching bands.[22,23] In particular the so-called Evans windows with intensity dips in the absorption bands are associated with Fermi resonances. Fermi resonances lead to absorption band splittings, where the coupling determines the splitting magnitude and the detuning governs the relative intensities of the different peaks.[10,11] The situation gets more complex when several Fermi resonances occur. In any case, coherent excitation of these splitted bands should lead to modulations in pump–probe signals that critically depend on the tuning of the excitation and probe pulses. Only when both bands of a Fermi doublet are simultaneously excited a coherent superposition occurs. One would expect that variation of the excitation frequency of the pulses only leads to changes in amplitude of the oscillations, whereas the phase remains equal to zero. If several Fermi resonances would occur with different coupling strengths and detuning parameters, the oscillatory contributions to the pump-probe signals should reveal a complex behaviour in frequency and amplitude.

Refering to our case of PMME-H (Table 1) we see that the $v = 2$ state of the O–H bending mode 40 lies 374 cm^{-1} below the O–H stretching mode 57, if we neglect the anharmonicity of the O–H bending mode. For PMME-D a calculated detuning value of 303 cm^{-1} is found. However, because of the extreme width of the O–H/O–D stretching band partial overlap

Table 1. Experimental (> 1000 cm^{-1}: in C_2Cl_4, < 1000 cm^{-1}: in KBr) and Calculated (B3LYP/6-31+G(d,p), Scaled by $f = 0.975$) Vibrational Frequencies of PMME-H and PMME-D (in cm^{-1})

No.[a]	PMME-H		PMME-D		Assignment[b]
	Experimental	Calculated	Experimental	Calculated	
57	≈ 3400–2500	3150	2500–2000	2311	ν(O–H/D)
56, 55		3108, 3104	3076, 3028,	3108, 3104,	$\nu(C–H)_{aromat.}$
54, 53		3080, 3066	2999	3080, 3066	$\nu(C–H)_{aromat.}$
52, 51		3060, 3031		3060, 3031	$\nu(CH_3)_{asym}$
50	2952	2950	2951	2950	$\nu(CH_3)_{sym}$
49	1743	1724	1742	1714	$\nu(C=O)_{carboxy}$
48	1704	1652	1701	1650	$\nu(C=O)_{ester}$
47	1602	1578	1602	1577	ν(ph-8*b*)
46	1581	1546	1581	1546	ν(ph-8*a*)
45	1493	1453	1491	1452	ν(ph-19*b*)
44, 43	1450	1438 + 1429	1450	1438 + 1429	$\delta(CH_3)_{asym}$
42	1434	1419	1433	1418	$\delta(CH_3)_{sym}$
41		1413		1412	ν(ph-19*a*) + δ(CH-3)
40	1412	1388	1045	1004	δ(O–H/D)
			1362		
39		1295		1296	ν(ph-14)
38	1293[c]	1255	1293	1255	$\nu(C–O)_{ester}$ + ν(C–COOH/D)
37	1280[c]	1253	1280	1243	δ(CH-3) + δ(O–H/D)
36	1261	1230	1261	1278	ν(C–OH/OD) + ν(C–COOH/D)
35	1192	1169	1194	1169	$\delta(CH_3)_{asym}$
34		1148		1148	δ(CH-9*a*)
33		1126		1125	$\delta(CH_3)_{asym}$
32	1143	1120	1143	1120	δ(CH-18*a*) + $\delta(CH_3)_{asym}$
31	1124	1100	1124	1103	δ(CH-18*b*)
30	1076	1051	1076	1052	δ(ph-12)
29	1040	1030	1040	1031	δ(ph-1)
28		977		977	γ(CH-5)
27	960	954		954	γ(CH-17*b*)
26	924	943		942	$\nu(O–CH_3)$
25		874		874	γ(CH-17*a*)
24	837[d]	840		595	γ(O–H/D)
23	806[d]	814		819	$\nu(C–COOCH_3)$ + γ(O–H/D) + $\delta(O=C–OCH_3)$
22	775[d]	777		777	γ(CH-11)−δ(COOH/D) + $\delta(COOCH_3)$
21	750[d]	763		755	ν(C–COOH/D)+ ν(O=C–OH/D)
20	702[d]	753		758	δ(COOH/D) + $\delta(COOCH_3)$
19	687[d]	706		706	γ(CH-11) + δ(COOH) + $\delta(COOCH_3)$
18	650[d]	666		665	δ(ph-6*b*)
17		653		657	γ(ph-4)
16		626		623	δ(ph-6*a*)
15	565	546		544	γ(ph-16*a*)
14	546	476		468	γ(ph-16*b*) + δ(–OH/D···O=C)
13		429		428	γ(ph-16*a*)
12		411		409	γ(ph-16*b*)−δ(–OH/D···O=C)
11		374		374	$\delta(O=C–OCH_3)$
10		343		342	ν(–O–H/D···O=C–) (15)
9		313		310	$\delta(COOCH_3)$ (9*b*)
8		267		264	δ(COOH/D) (9*b*)
7		219		219	$\tau(C–OCH_3)$ + 10*a*
6		172		171	$\delta(OCH_3)$
5		147		147	$\tau(CH_3)$
4		125		125	$\tau(CH_3)$
3		88		88	$\gamma(Subs.\text{-}torsion)_{sym}$(10*b*)
2		69		68	$\gamma(Subs.\text{-}torsion)_{asym}$
1		36		35	$\gamma(Subs.\text{-}torsion)_{sym}$

a) The numbering refers to calculated frequencies for PMME-H. b) ν = stretching, δ = in-plane deformation, γ = out-of-plane deformation, τ = torsion. Varsanyi nomenclature where applicable. c) These two modes cannot be discriminated. d) These modes cannot be assigned unambiguously.

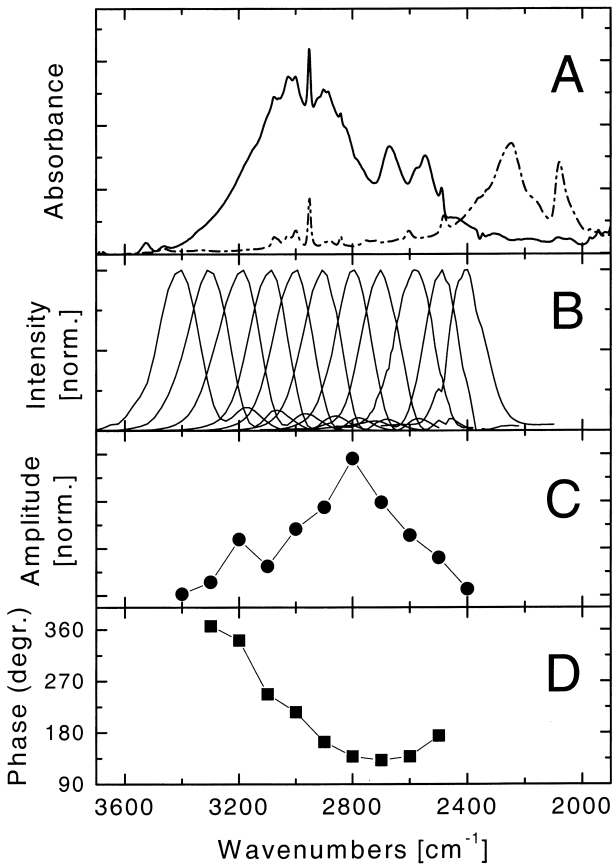

Fig. 4. (A): Absorption spectrum of PMME-H in C_2Cl_4. The spectrum of PMME-D is also shown for comparison (dotted line). The remaining peaks in the 3000 cm^{-1} are small bands due to C–H stretching modes of PMME. (B): Spectra of the mid-infrared laser pulses. (C): Amplitude of the 100 cm^{-1} oscillatory contribution to the pump-probe signal. (D): Initial phase of the oscillatory contribution.

with the overtone state of the O–H/O–D bending mode might be possible. In fact, the intensity dips in O–H/O–D stretching bands (Fig. 4A) may be an indication for the occurrence of Fermi resonances, in particular for PMME-D.

The O–H stretching band of PMME-H is about two times as broad as the O–D band in PMME-D. Because of this we are able to explore the laser tuning dependency of coherent response of PMME-H with spectrally integrated ("open band") single-colour pump–probe spectroscopy. The coherent contribution is present throughout the absorption band of PMME-H with the same single frequency and with a gradual change of amplitude, as well as an overall change in phase of 200–230 degrees (Figs. 4C and D). From this observation we exclude the possible contribution of the Fermi resonance to the oscillatory contribution in the pump–probe signals. We conclude that the coherent modulations are due to anharmonic coupling of the O–H/O–D stretching mode to the low-frequency out-of-plane mode 2 from Table 1. The frequency of this oscillatory mode in PMME-H, 100 cm^{-1}, is identical to that observed for PMME-D,[12] as expected from the normal mode calculations.

Coherent motion of vibrational wave packets of low-frequency modes have been observed since ultrafast lasers have been used in numerous studies on vibronic transitions. Impulsive stimulated Raman scattering with excitation off-resonant with respect to electronic transitions lead to the coherent preparation of wave packets in the electronic ground state.[24–26] Excitation resonant with electronic transitions leads to the impulsive preparation of wave packets both in the electronic ground and in the excited states,[27] where the efficiency for the latter process is usually more efficient for the case of long electronic excited state lifetimes.[28–30] When the excited state lifetime is short compared to the coherence decay times of the wave packet motions the ground state contributions to the observed signals become more dominant.[31] In addition, vibrational coherent wave packet motion has also been observed for cases where the coherence is driven by rapid nonradiative processes, where the wave packets are observed in product states.[32–36]

In the present work we present data of coherent vibrational wave packet motions of the out-of-plane mode of PMME-H generated by ultrashort mid-IR pulses in the electronic ground state. When the adiabatic separation of time scales between the O–H stretching and the low-frequency modes is made, we expect by analogy with electronic spectroscopy that both in the $v = 1$ and in the $v = 0$ states of the O–H stretching vibration these wave packet motions occur. In the reported work on PMME-D we used singular value decompositon to derive the spectral profile associated with the oscillatory contribution to the pump-probe signal. We have not been able to distinguish components due to motion in the excited $v = 1$ and in the ground $v = 0$ O–D stretching states for the case of PMME-D. We note that we observed solely ground-state vibrational wave packet motion in 2-(2′-hydroxyphenyl)benzothiazole where the excited lifetime is much shorter than the coherence decay of the wave packet.[37] If the T_1-lifetime of the $v = 1$ state is much shorter than 200 fs, the data obtained on PMME-H show a dominant contribution of ground state vibrational wave packet dynamics as well. In principle, one cannot exclude that coherent motion continues when the excited $v = 1$ state decays to the relaxed "hot" spectrally blue-shifted $v = 0'$ state. On the other hand, if the coherence is only (partially) preserved during the T_1-relaxation, the overall damping factor of the oscillations will be attenuated compared to the case of a sole contribution from a $v = 0$ ground state wave packet. It thus appears to be an important question to solve whether coherence of the low-frequency mode is transferred into the $v = 0'$ state.

The derived results on the amplitude and phase of the coherent modulations of the pump–probe signals (Figs. 4C and D) indicate that a simple two-level model with respect to the O–H stretching mode does not fully apply for the case of PMME-H. This conclusion can be drawn by comparison to recent work by the Champion group on femtosecond coherence spectroscopy.[38] Amongst various cases they report on the amplitude and phase properties of a two level electronic system consisting of a linearly displaced harmonic oscillator. When performing the spectrally integrated ("open band") single colour pump–probe spectroscopy a distinctive phase flip of 180 degrees occurs for the ground state wave packet around the absorption maximum. By scanning over the whole band a total phase change of 360 degrees occurs, whereas the phase flip for the excited state wave packet near the emission maximum is 180 degrees. The amplitude of the oscillatory contribution to the pump-probe

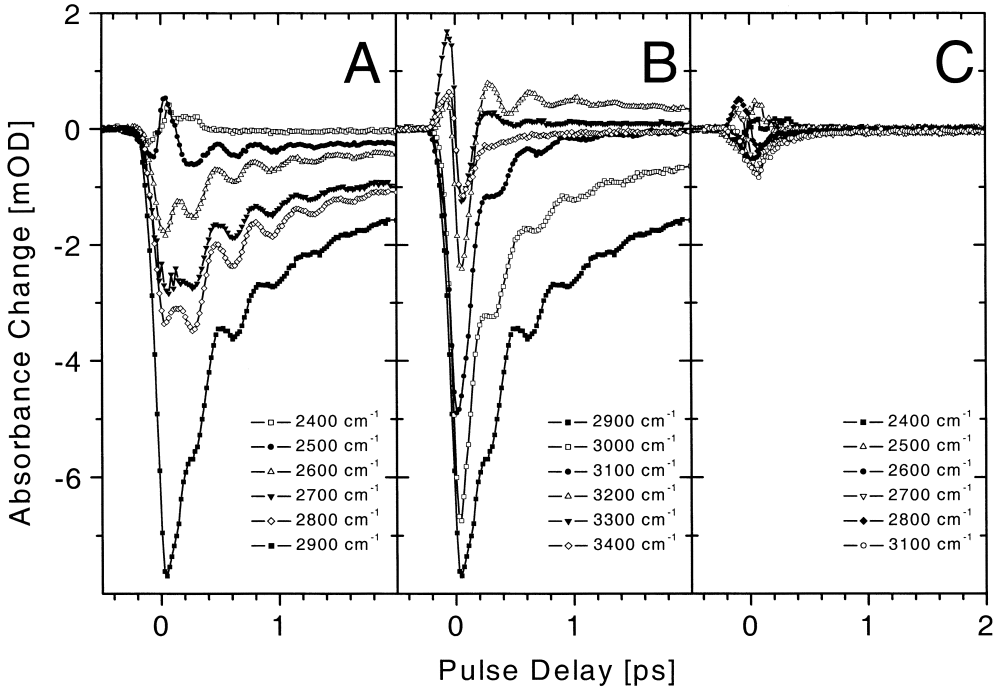

Fig. 5. Pump–probe data of PMME-H in C_2Cl_4 (A) and (B) and pure solvent signal (C) depicted at ordinary scale, showing the bleach, stimulated emission, and transient absorption signals together with the oscillatory contribution.

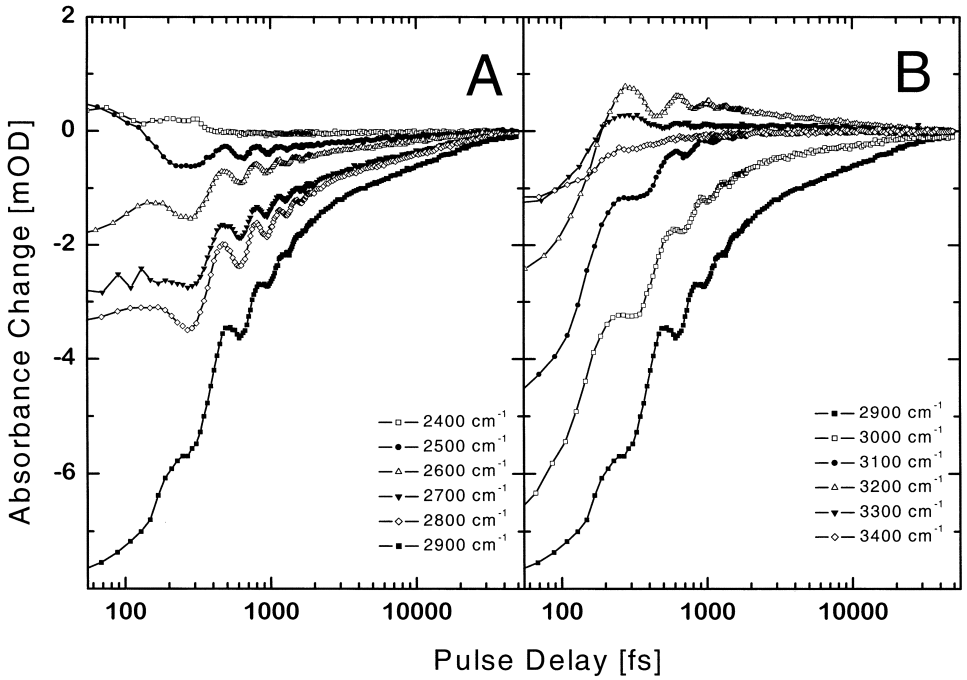

Fig. 6. Pump–probe data of PMME-H in C_2Cl_4 (A and B) depicted at log scale along the time axis, showing the (non-exponential) relaxation to the ground state at picosecond time scales.

signal diminishes to zero where the phase flip occurs.

In the case of PMME-H an amplitude "dip" might be present that occurs around 3100 cm^{-1}, at the maximum of the O–H stretching band. This observation hints that at this spectral position the origin (0–0) transition of the O–H stretching band should be located, if the two-level system is valid that is based on the adiabatic separation of time scales between the high-frequency O–H stretching and the low-frequency out-of-plane O···O mode. However, such a conclusion cannot be drawn in full confidence, since the "dip" is not pronounced.

The observed phase change in the region around 3100 cm^{-1} is more gradual and appears to be larger than 180 degrees. If we assume that the wave packet dynamics are similar to that of vibronic transitions, then the more gradual change points to the

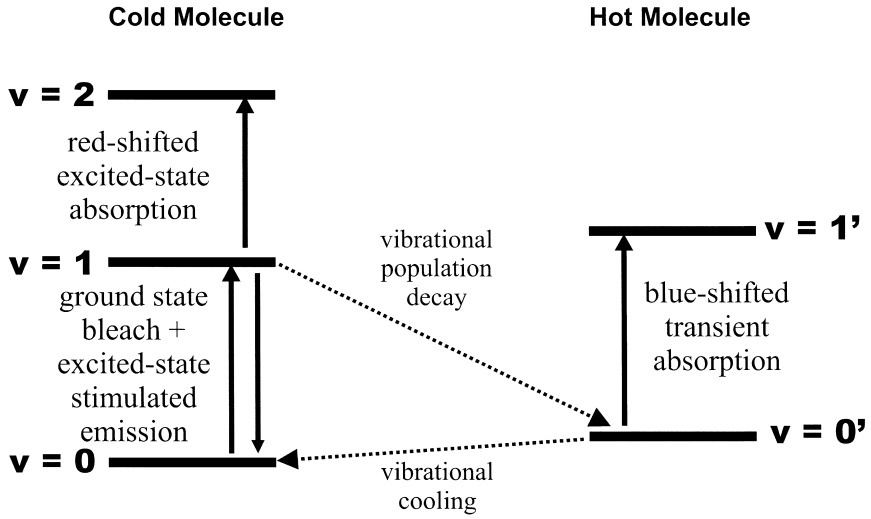

Fig. 7. Level structure implementing the $v = 0$, $v = 1$ and $v = 2$ states of the O–H stretching mode, as well as two levels of the "hot" molecule that shows up when the $v = 1$ state decays.

fact that at room temperature the motion of the out-of-plane mode is not in the high temperature limit, consistent with the simulations by Champion and co-workers.[38] The fact that the overall phase change of the oscillations in the pump–probe signal, when scanning the excitation pulses over the O–H stretching band, varies over a range of 200–230 degrees would indicate that both ground state and excited state wave packets contribute significantly, as expected for the case of systems where the excited state lifetimes are in the same order of magnitude as the coherence decay times of the wave packet motions. A better estimate of the relative contributions of ground and excited wave packet motions might be made when the T_1-relaxation time has been determined accurately. The fact that the phase change occurs at the high frequency side of the O–H stretching band, and not in the centre, might indicate a deviation from the simple two-level system.

Conclusions

We have performed single-colour spectrally integrated mid-infrared pump-probe spectroscopy on the O–H stretching vibrational transition of phthalic acid monomethyl ester (PMME-H). With ultrashort mid-infrared laser pulses tuned to this vibrational transition we detect coherent modulations the hydrogen bond distance in PMME-H caused by impulsive excitation of a low-frequency out-of-plane mode. The frequency of this out-of-plane mode is identical as in the deuterated derivative PMME-D. We exclude the role of Fermi resonances as the underlying mechanism for the coherent modulations. We ascribe the observed oscillations to wave packet motions of an anharmonically coupled low frequency out-of-plane mode that modulates the hydrogen bond distance. The amplitude and phase dependencies of the coherent modulations in the pump-probe signals, as a function of the tuning frequency of the laser pulses, indicate that both ground and excited state wave packets have significant amplitude throughout the band. Several questions remain unsolved, such as a more accurate determination of the $v = 1$ excited state lifetime, and also the possibility of nonradiative coherence transfer when the $v = 1$ state relaxes to the "hot" blue-shifted $v = 0'$ state. These questions will be addressed by two colour pump–probe measurements on PMME-H.

The mid-infrared spectroscopic activities on hydrogen bonds in the electronic ground state are embedded in the collaborative research center *Analysis and Control of Photoinduced Reactions* (Sonderforschungsbereich 450 *Analyse und Steuerung ultraschneller photoinduzierter Reaktionen*), supported by the Deutsche Forschungsgemeinschaft. We cordially thank J. Manz, O. Kühn, H. Naundorf and G. K. Paramonov from the Freie Universität Berlin for stimulating discussions.

References

1 D. Hadži and S. Bratos, in "The Hydrogen Bond: Recent developments in theory and experiments, Vol. II. Structure and Spectroscopy," ed by P. Schuster, G. Zundel, and C. Sandorfy, North Holland, Amsterdam, the Netherlands (1976), pp. 565–611.

2 Y. Marechal and A. Witkowski, *J. Chem. Phys.*, **48**, 3697 (1968).

3 G. N. Robertson and J. Yarwood, *Chem. Phys.*, **32**, 267 (1978).

4 O. Henri-Rousseau and P. Blaise, *Adv. Chem. Phys.*, **103**, 1 (1998).

5 H. Abramczyk, *Chem. Phys.*, **94**, 91 (1985).

6 J. Stenger, D. Madsen, P. Hamm, E. T. J. Nibbering, and T. Elsaesser, *Phys. Rev. Lett.*, **87**, 027401 (2001).

7 J. Stenger, D. Madsen, P. Hamm, E. T. J. Nibbering, and T. Elsaesser, *J. Phys. Chem. A*, **106**, 2341 (2002).

8 J. Stenger, D. Madsen, J. Dreyer, P. Hamm, E. T. J. Nibbering, and T. Elsaesser, *Chem. Phys. Lett.*, "Femtosecond mid-infrared photon echo study of an intramolecular hydrogen bond," in press (2002).

9 G. K. Paramonov, H. Naundorf, and O. Kühn, *Eur. Phys. J. D*, **14**, 205 (2001).

10 O. Henri-Rousseau and D. Chamma, *Chem. Phys.*, **229**, 37 (1998).

11 D. Chamma and O. Henri-Rousseau, *Chem. Phys.*, **229**, 51

(1998).

12 J. Stenger, D. Madsen, J. Dreyer, E. T. J. Nibbering, P. Hamm, and T. Elsaesser, *J. Phys. Chem. A*, **105**, 2929 (2001).

13 P. Hamm, R. A. Kaindl, and J. Stenger, *Opt. Lett.*, **25**, 1798 (2000).

14 R. A. Kaindl, M. Wurm, K. Reimann, P. Hamm, A. M. Weiner, and M. Woerner, *J. Opt. Soc. Am. B*, **17**, 2086 (2000).

15 M. J. Frisch, G. W. Trucks, H. B. Schlegel, G. E. Scuseria, M. A. Robb, J. R. Cheeseman, V. G. Zakrzewski, J. A. Montgomery, R. E. Stratmann, J. C. Burant, S. Dapprich, J. M. Millam, A. D. Daniels, K. N. Kudin, M. C. Strain, O. Farkas, J. Tomasi, V. Barone, M. Cossi, R. Cammi, B. Mennucci, C. Pomelli, C. Adamo, S. Clifford, J. Ochterski, G. A. Petersson, P. Y. Ayala, Q. Cui, K. Morokuma, D. K. Malick, A. D. Rabuck, K. Raghavachari, J. B. Foresman, J. Cioslowski, J. V. Ortiz, B. B. Stefanov, G. Liu, A. Liashenko, P. Piskorz, I. Komaromi, R. Gomperts, R. L. Martin, D. J. Fox, T. Keith, M. A. Al-Laham, C. Y. Peng, A. Nanayakkara, C. Gonzalez, M. Challacombe, P. M. W. Gill, B. G. Johnson, W. Chen, M. W. Wong, J. L. Andres, M. Head-Gordon, E. S. Replogle, and J. A. Pople, "Gaussian 98 (Revision A.2)," Gaussian, Inc., Pittsburgh PA. (1998).

16 A. P. Scott and L. Radom, *J. Phys. Chem.*, **100**, 16502 (1996).

17 G. A. Jeffrey, "Introduction to Hydrogen Bonding," Oxford University Press, Oxford (1997).

18 P. Hamm and R. M. Hochstrasser, in "Ultrafast infrared and Raman spectroscopy," ed by M. D. Fayer, Marcel Dekker, Inc., New York (2001), pp. 273–347.

19 A. J. Lock, S. Woutersen, and H. J. Bakker, *J. Phys. Chem. A*, **105**, 1238 (2001).

20 H. Graener, T. Q. Ye, and A. Laubereau, *J. Chem. Phys.*, **90**, 3413 (1989).

21 G. R. Fleming, "Chemical applications of ultrafast spectroscopy," Oxford University Press, Oxford (1986).

22 S. Bratos, *J. Chem. Phys.*, **63**, 3499 (1975).

23 S. Bratos and H. Ratajczak, *J. Chem. Phys.*, **76**, 77 (1982).

24 T. P. Dougherty, G. P. Wiederrecht, K. A. Nelson, M. H. Garrett, H. P. Jensen, and C. Warde, *Science*, **258**, 770 (1992).

25 L. Dhar, J. A. Rogers, and K. A. Nelson, *Chem. Rev.*, **94**, 157 (1994).

26 G. Korn, O. Dühr, and A. Nazarkin, *Phys. Rev. Lett.*, **81**, 1215 (1998).

27 W. T. Pollard and R. A. Mathies, *Ann. Rev. Phys. Chem.*, **43**, 497 (1992).

28 M. J. Rosker, F. W. Wise, and C. L. Tang, *Phys. Rev. Lett.*, **57**, 321 (1986).

29 A. H. Zewail, *Science*, **242**, 1645 (1988).

30 H. L. Fragnito, J. Y. Bigot, P. C. Becker, and C. V. Shank, *Chem. Phys. Lett.*, **160**, 101 (1989).

31 M. H. Vos, F. Rappaport, J.-C. Lambry, J. Breton, and J.-L. Martin, *Nature*, **363**, 320 (1993).

32 M. Dantus, R. M. Bowman, M. Gruebele, and A. H. Zewail, *J. Chem. Phys.*, **91**, 7437 (1989).

33 U. Banin, A. Waldman, and S. Ruhman, *J. Chem. Phys.*, **96**, 2416 (1992).

34 N. Pugliano, D. K. Palit, A. Z. Szarka, and R. M. Hochstrasser, *J. Chem. Phys.*, **99**, 7273 (1993).

35 Q. Wang, R. W. Schoenlein, L. A. Peteanu, R. A. Mathies, and C. V. Shank, *Science*, **266**, 422 (1994).

36 L. Zhu, J. T. Sage, and P. M. Champion, *Science*, **266**, 629 (1994).

37 D. Madsen, J. Stenger, J. Dreyer, E. T. J. Nibbering, P. Hamm, and T. Elsaesser, *Chem. Phys. Lett.*, **341**, 56 (2001).

38 A. T. N. Kumar, F. Rosca, A. Widom, and P. M. Champion, *J. Chem. Phys.*, **114**, 701 (2001).